

Axisymmetric equilibria with pressure anisotropy and plasma flow

A. Evangelias^{1,a)}, G. N. Throumoulopoulos^{1,a)}

¹*University of Ioannina, Physics Department,*

Section of Astrogeophysics, GR 451 10 Ioannina, Greece

^{a)}*Electronic Addresses: aevag@cc.uoi.gr, gthroum@cc.uoi.gr*

A generalised Grad-Shafranov equation that governs the equilibrium of an axisymmetric toroidal plasma with anisotropic pressure and incompressible flow of arbitrary direction is derived. This equation includes six free surface functions and recovers known Grad-Shafranov-like equations in the literature as well as the usual static, isotropic one. The form of the generalised equation indicates that pressure anisotropy and flow act additively on equilibrium. In addition, two sets of analytical solutions, an extended Solovév one with a plasma reaching the separatrix and an extended Hernegger-Maschke one for a plasma surrounded by a fixed boundary possessing an X-point, are constructed, particularly in relevance to the ITER and NSTX tokamaks. Furthermore, the impacts both of pressure anisotropy and plasma flow on these equilibria are examined. It turns out that depending on the maximum value and the shape of an anisotropy function, the anisotropy can act either paramagnetically or diamagnetically. Also, in most of the cases considered both the anisotropy and the flow have stronger effects on NSTX equilibria than on ITER ones.

I. INTRODUCTION

It has been established in a number of fusion devices that sheared flow both zonal and mean (equilibrium) play a role in the transitions to improved confinement regimes as the L-H transition and the Internal Transport Barriers [1], [2]. These flows can be driven externally in connection with electromagnetic power and neutral beam injection for plasma heating and current drive or can be created spontaneously (zonal flow). An additional effect of external heating, depending on the direction of the injected momentum, is pressure anisotropy which also may play a role in several magnetic fusion related problems.

In many important plasmas as the high temperature ones the collision time is so long that collisions can be ignored. It would appear that for such collisionless plasmas a fluid theory should not be appropriate. However, for perpendicular motions because of gyromotion the magnetic field plays the role of collisions, thus making a fluid description appropriate. Macroscopic equations for a collisionless plasma with pressure anisotropy have been derived by Chew, Goldberger, and Low [3] on the basis of a diagonal pressure tensor consisting of

one element parallel to the magnetic field and a couple of identical perpendicular elements associated with two degrees of freedom.

The MHD equilibria of axisymmetric plasmas, which can be starting points of stability and transport studies, is governed by the well known Grad-Shafranov (GS) equation. The most widely employed analytic solutions of this equation is the Solovév solution [4] and the Hernegger-Maschke solution [5], the former corresponding to toroidal current density non vanishing on the plasma boundary and the latter to toroidal current density vanishing thereon. In the presence of flow the equilibrium satisfies a generalised Grad-Shafranov (GGS) equation together with a Bernoulli equation involving the pressure (see for example [6–8]). For compressible flow the GGS equation can be either elliptic or hyperbolic depending on the value of a Mach function associated with the poloidal velocity. Note that the toroidal velocity is inherently incompressible because of axisymmetry. In the presence of compressibility the GGS equation is coupled with the Bernoulli equation through the density which is not uniform on magnetic surfaces. For incompressible flow the density becomes a surface quantity and the GGS equation becomes elliptic and decouples from the Bernoulli equation (see section II). Consequently one has to solve an easier and well posed elliptic boundary value problem. In particular for fixed boundaries, convergence to the solution is guaranteed under mild requirements of monotonicity for the free functions involved in the GGS equation [9]. For plasmas with anisotropic pressure the equilibrium equations involve a function associated with this anisotropy [Eq. (8) below]. To get a closed set of reduced equilibrium equations an assumption on the functional dependence of this function is required (cf. [10]–[16] for static equilibria and [17]–[23] for stationary ones).

In this work we derive a new GGS equation by including both anisotropic pressure and incompressible flow of arbitrary direction. This equation consists of six arbitrary surface quantities and recovers known equations as particular cases, as well as the usual GS equation for a static isotropic plasma. Together we obtain a Bernoulli equation for the quantity \bar{p} [Eq. (9)], which may be interpreted as an effective isotropic pressure. For the derivation we assume that the function of pressure anisotropy is uniform on magnetic surfaces. In fact, as it will be shown, for static equilibria as well as for stationary equilibria either with toroidal flow or incompressible flow parallel to the magnetic field, this property of the anisotropy function follows if the current density shares the same surfaces with the magnetic field. Then for appropriate choices of the free functions involved we obtain an extended Solovév solution describing configurations with a non-predefined boundary, and an extended Hernegger-Maschke solution with a fixed boundary possessing an X-point imposed by Dirichlet boundary conditions. On the basis of these solutions we construct ITER-like, as well as NSTX and NSTX-Upgrade-like equilibria for arbitrary flow, both diamagnetic and paramagnetic, to examine the impact both of pressure anisotropy and plasma flow on the equilibrium characteristics. The main conclusions are that the pressure anisotropy and the flow act on equilibrium in an additive way, with the anisotropy having a stronger impact than that of the flow. Also the effects of flow and anisotropy are in general more noticeable in spherical tokamaks than in conventional ones.

The GGS equation for plasmas with pressure anisotropy and flow is derived in section II. In section III the generalised Solovév and Hernegger-Maschke solutions are obtained and employed to construct ITER and NSTX pertinent configurations. Then the impact of anisotropy and flow on equilibrium quantities, as the pressure and current density, are examined in section IV. Section V summarizes the conclusions.

II. THE GENERALISED GRAD-SHAFRANOV EQUATION

The ideal MHD equilibrium states of an axially symmetric magnetically confined plasma with incompressible flow and anisotropic pressure are governed by the following set of equations:

$$\vec{\nabla} \cdot (\rho \vec{v}) = 0 \quad (1)$$

$$\rho(\vec{v} \cdot \vec{\nabla})\vec{v} = \vec{J} \times \vec{B} - \vec{\nabla} \cdot \overset{\leftrightarrow}{\mathbb{P}} \quad (2)$$

$$\vec{\nabla} \times \vec{B} = \mu_0 \vec{J} \quad (3)$$

$$\vec{\nabla} \times \vec{E} = 0 \quad (4)$$

$$\vec{\nabla} \cdot \vec{B} = 0 \quad (5)$$

$$\vec{E} + \vec{v} \times \vec{B} = 0 \quad (6)$$

The diagonal pressure tensor $\overset{\leftrightarrow}{\mathbb{P}}$, introduced in [3], consists of one element parallel to the magnetic field, p_{\parallel} , and two equal perpendicular ones, p_{\perp} , and is expressed as

$$\overset{\leftrightarrow}{\mathbb{P}} = p_{\perp} \overset{\leftrightarrow}{\mathbb{I}} + \frac{\sigma_d}{\mu_0} \vec{B} \vec{B} \quad (7)$$

where the dimensionless function

$$\sigma_d = \mu_0 \frac{p_{\parallel} - p_{\perp}}{|\vec{B}|^2} \quad (8)$$

is a measure of the pressure anisotropy. Particle collisions in equilibrating parallel and perpendicular energies will reduce σ_d and therefore a collision-dominated plasma can be described accurately by a scalar pressure. However, because of the low collision frequency a high-temperature confined plasma remains for long anisotropic, once anisotropy is induced by external heating sources.

At this point we define the quantity

$$\bar{p} = \frac{p_{\parallel} + p_{\perp}}{2} \quad (9)$$

which may be interpreted as an effective isotropic pressure, and which should not be confused with the average plasma pressure

$$\langle p \rangle = \frac{1}{3} \text{Tr}(\overset{\leftrightarrow}{\mathbb{P}}) = \frac{p_{\parallel} + 2p_{\perp}}{3} = \bar{p} - \sigma_d \frac{B^2}{6\mu_0} \quad (10)$$

On the basis of Eqs. (8) and (9), the following instructive relations arise for the two scalar pressures:

$$p_{\perp} = \bar{p} - \sigma_d \frac{B^2}{2\mu_0} \quad (11)$$

and

$$p_{\parallel} = \bar{p} + \sigma_d \frac{B^2}{2\mu_0} \quad (12)$$

Owing to axisymmetry, the divergence-free fields, i.e., the magnetic field, the current density, \vec{J} , and the momentum density of the fluid element, $\rho\vec{v}$, can be expressed in terms of the stream functions $\psi(R, z)$, $I(R, z)$, $F(R, z)$ and $\Theta(R, z)$ as

$$\vec{B} = I\vec{\nabla}\phi + \vec{\nabla}\phi \times \vec{\nabla}\psi \quad (13)$$

$$\vec{J} = \frac{1}{\mu_0}(\Delta^*\psi\vec{\nabla}\phi - \vec{\nabla}\phi \times \vec{\nabla}I) \quad (14)$$

and

$$\rho\vec{v} = \Theta\vec{\nabla}\phi + \vec{\nabla}\phi \times \vec{\nabla}F \quad (15)$$

Here, (R, ϕ, z) denote the usual right-handed cylindrical coordinate system; constant ψ surfaces are the magnetic surfaces; F is related to the poloidal flux of the momentum density field, $\rho\vec{v}$; the quantity $I = RB_{\phi}$ is related to the net poloidal current flowing in the plasma and the toroidal field coils; $\Theta = \rho Rv_{\phi}$; Δ^* is the elliptic operator defined by $\Delta^* \equiv R^2\vec{\nabla} \cdot (\vec{\nabla}/R^2)$; and $\vec{\nabla}\phi \equiv \hat{e}_{\phi}/R$.

Equations (1)-(6) can be reduced by means of certain integrals of the system, which are shown to be surface quantities. To identify two of these quantities, the time independent electric field is expressed by $\vec{E} = -\vec{\nabla}\Phi$ and the Ohm's law, (6), is projected along $\vec{\nabla}\phi$ and \vec{B} , respectively, yielding

$$\vec{\nabla}\phi \cdot (\vec{\nabla}F \times \vec{\nabla}\psi) = 0 \quad (16)$$

and

$$\vec{B} \cdot \vec{\nabla}\Phi = 0 \quad (17)$$

Equations (16) and (17) imply that $F = F(\psi)$ and $\Phi = \Phi(\psi)$. An additional surface quantity is found from the component of Eq. (6) perpendicular to a magnetic surface:

$$\Phi' = \frac{1}{\rho R^2}(IF' - \Theta) \quad (18)$$

where the prime denotes differentiation with respect to ψ . On the basis of Eq. (18) the velocity [Eq. (15)] can be written in the form

$$\vec{v} = \frac{F'}{\rho}\vec{B} - R^2\Phi'\vec{\nabla}\psi \quad (19)$$

Thus, \vec{v} is decomposed into a component parallel to \vec{B} and a non parallel one associated with the electric field in consistence with the Ohm's law (6). Subsequently, by projecting Eq. (2) along $\vec{\nabla}\psi$ we find a fourth surface quantity of the system:

$$X(\psi) \equiv (1 - \sigma_d - M_p^2)I + \mu_0 R^2 F' \Phi' \quad (20)$$

Here we have introduced the poloidal Mach function as:

$$M_p^2 \equiv \mu_0 \frac{(F')^2}{\rho} = \frac{v_{pol}^2}{B_{pol}^2/\mu_0\rho} = \frac{v_{pol}^2}{v_{Apol}^2} \quad (21)$$

where $v_{Apol} = \frac{B_{pol}}{\sqrt{\mu_0\rho}}$ is the Alfvén velocity associated with the poloidal magnetic field. From Eqs. (18) and (20) it follows that, neither I is a surface quantity, unlike the case of static, isotropic equilibria, nor Θ .

With the aid of Eqs. (16)-(19) and (20), the components of Eq. (2) along \vec{B} and perpendicular to a magnetic surface are put in the respective forms

$$\vec{B} \cdot \left\{ \vec{\nabla} \left[\frac{v^2}{2} + \frac{\Theta\Phi'}{\rho} \right] + \frac{1}{\rho} \vec{\nabla} p \right\} = 0 \quad (22)$$

and

$$\begin{aligned} & \left\{ \vec{\nabla} \cdot \left[(1 - \sigma_d - M_p^2) \frac{\vec{\nabla}\psi}{R^2} \right] + \left[\mu_0 \frac{F'F''}{\rho} - (1 - \sigma_d)' \right] \frac{|\vec{\nabla}\psi|^2}{R^2} - \mu_0 \sigma_d' \frac{B^2}{2\mu_0} \right\} |\vec{\nabla}\psi|^2 \\ & + \left\{ \mu_0 \rho \vec{\nabla} \left(\frac{v^2}{2} \right) - \frac{\mu_0 \rho}{2R^2} \vec{\nabla} \left(\frac{\Theta}{\rho} \right)^2 + \frac{(1 - \sigma_d)}{2R^2} \vec{\nabla} I^2 + \mu_0 \vec{\nabla} p \right\} \cdot \vec{\nabla}\psi = 0 \end{aligned} \quad (23)$$

Therefore, irrespective of compressibility the equilibrium is governed by the equations (22) and (23) coupled through the density, ρ , and the pressure anisotropy function, σ_d . Equation (23) has a singularity when $\sigma_d + M_p^2 = 1$, and so we must assume that $\sigma_d + M_p^2 \neq 1$.

In order to reduce the equilibrium equations further, we employ the incompressibility condition

$$\vec{\nabla} \cdot \vec{v} = 0 \quad (24)$$

Then Eq. (1) implies that the density is a surface quantity,

$$\rho = \rho(\psi) \quad (25)$$

and so is the Mach function

$$M_p^2 = M_p^2(\psi) \quad (26)$$

In addition to obtain a closed set of equations following [10, 11, 16, 20] we assume that σ_d is uniform on magnetic surfaces

$$\sigma_d = \sigma_d(\psi) \quad (27)$$

For static equilibria this follows from Eq. (20), which becomes $X(\psi) = -I\sigma_d$, if in the presence of anisotropy the current density remains on the magnetic surfaces ($I = I(\psi)$). Since $M_p = M_p(\psi)$, the same implication for σ_d holds for parallel incompressible flow as well

as for toroidal flow. Also, the hypothesis $\sigma_d = \sigma_d(\psi)$, according to [10], may be the only suitable for satisfying the boundary conditions on a rigid, perfectly conducting wall.

From Eqs. (18) and (20) it follows that axisymmetric equilibria with purely poloidal flow ($\Theta = 0$) cannot exist because of the following contradiction: from Eq. (20) it follows that $I = \frac{X(\psi)}{1-\sigma_d(\psi)}$ is a surface function, but also, $I = \frac{\rho(\psi)\Phi'(\psi)}{F'(\psi)}R^2$ from Eq. (18), implying that I has an explicit dependence on R ; so it cannot be a surface function. On the other hand, there can exist an equilibrium with purely toroidal flow, either “compressible”, in the sense that the density varies on the magnetic surfaces, or an incompressible one with uniform density $\rho(\psi)$ thereon. For isotropic plasmas both kinds of these equilibria were examined in [24].

With the aid of Eq. (25), Eq. (22) can be integrated to yield an expression for the effective pressure, i.e.,

$$\bar{p} = \bar{p}_s(\psi) - \rho \left[\frac{v^2}{2} - \frac{(1 - \sigma_d)R^2(\Phi')^2}{1 - \sigma_d - M_p^2} \right] \quad (28)$$

Therefore, in the presence of flow the magnetic surfaces in general do not coincide with the surfaces on which \bar{p} is uniform. In this respect, the term containing $\bar{p}_s(\psi)$ is the static part of the effective pressure which does not vanish when $\vec{v} = 0$.

Finally, by inserting Eq. (28) into Eq. (23) after some algebraic manipulations, the latter reduces to the following elliptic differential equation,

$$\begin{aligned} & (1 - \sigma_d - M_p^2)\Delta^* \psi + \frac{1}{2}(1 - \sigma_d - M_p^2)' |\vec{\nabla} \psi|^2 + \frac{1}{2} \left(\frac{X^2}{1 - \sigma_d - M_p^2} \right)' \\ & + \mu_0 R^2 \bar{p}_s' + \mu_0 \frac{R^4}{2} \left[\frac{(1 - \sigma_d)\rho(\Phi')^2}{1 - \sigma_d - M_p^2} \right]' = 0 \end{aligned} \quad (29)$$

This is the GGS equation that governs the equilibrium for an axisymmetric plasma with pressure anisotropy and incompressible flow. For flow parallel to the magnetic field the R^4 -term vanishes. For vanishing flow Eq. (29) reduces to the one derived in [11], when the pressure is isotropic it reduces to the one obtained in [8], and when both anisotropy and flow are absent it reduces to the well known GS equation. Equation (29) contains six arbitrary surface quantities, namely: $X(\psi)$, $\Phi(\psi)$, $\bar{p}_s(\psi)$, $\rho(\psi)$, $M_p^2(\psi)$ and $\sigma_d(\psi)$, which can be assigned as functions of ψ to obtain analytically solvable linear forms of the equation or from other physical considerations.

A. Isodynamicity

There is a special class of static equilibria called isodynamic for which the magnetic field magnitude is a surface quantity ($|\vec{B}| = |\vec{B}(\psi)|$) [25]. This feature can have beneficial effects on confinement because the grad- B drift vanishes and consequently plasma transport perpendicular to the magnetic surfaces is reduced. Also, it was proved that the only possible isodynamic equilibrium is axisymmetric [26]. For fusion plasmas the thermal conduction along \vec{B} is fast compared to the heat transport perpendicular to a magnetic surface, so a good assumption is that the parallel temperature is a surface function, $T_{\parallel} = T_{\parallel}(\psi)$. Then, assuming that the plasma obeys the ideal gas law, it follows that the parallel pressure becomes also a surface function, $p_{\parallel} = p_{\parallel}(\psi)$.

With the aid of these assumptions, and on the basis of Eqs. (19) and (22) it follows that the magnitude of the magnetic field is related with the perpendicular pressure as

$$|\vec{B}|^2 = \frac{2G(\psi)}{M_p^2(\psi)} - \left(p_\perp - \rho R^2 (\Phi')^2 \right) \frac{1}{M_p^2(\psi)} \quad (30)$$

where $G(\psi) \equiv \rho \left[\frac{v^2}{2} + \frac{\Theta \Phi'}{\rho} \right] + \frac{p_\perp}{2}$. We note that $|\vec{B}|^2$ becomes a surface function when the perpendicular pressure satisfies the relation $p_\perp = \rho R^2 (\Phi')^2$. This implies that

$$\sigma_d = \sigma_d(\psi, R) = \mu_0 \frac{p_\parallel(\psi)}{|\vec{B}|^2(\psi)} - R^2 \mu_0 \frac{\rho(\psi) (\Phi')^2(\psi)}{|\vec{B}|^2(\psi)} \quad (31)$$

which is in contradiction with the hypothesis that the function σ_d is a surface quantity. Consequently, the only possibility for isodynamic magnetic surfaces to exist is that for field aligned flow, $\Phi' = 0$, because then Eq. (30) reduces to

$$|\vec{B}|^2 = \frac{2G(\psi)}{M_p^2(\psi)} - \frac{p_\perp}{M_p^2(\psi)} \quad (32)$$

Eqs. (8) and (32) imply that both $|\vec{B}|^2 = |\vec{B}|^2(\psi)$ and $p_\perp = p_\perp(\psi)$.

Thus, the conclusions for the isotropic case [8] are generalised for anisotropic pressure, i.e. all three B , p_\parallel and p_\perp become surface quantities. We note here that the more physically pertinent case that B and p_\perp remain arbitrary functions would require either compressibility or eliminating the assumption $\sigma_d = \sigma_d(\psi)$. However, in this case tractability is lost and the problem requires numerical treatment.

B. Generalised Transformation

Using the transformation

$$u(\psi) = \int_0^\psi \sqrt{1 - \sigma_d(g) - M_p^2(g)} dg, \quad \sigma_d + M_p^2 < 1 \quad (33)$$

Eq. (29) reduces to

$$\Delta^* u + \frac{1}{2} \frac{d}{du} \left(\frac{X^2}{1 - \sigma_d - M_p^2} \right) + \mu_0 R^2 \frac{d\bar{p}_s}{du} + \mu_0 \frac{R^4}{2} \frac{d}{du} \left[(1 - \sigma_d) \rho \left(\frac{d\Phi}{du} \right)^2 \right] = 0 \quad (34)$$

Transformation (33) does not affect the magnetic surfaces, it just relabels them by the flux function u , and is a generalisation of that introduced in [27] for isotropic equilibria with incompressible flow ($\sigma_d = 0$) and that introduced in [11] for static anisotropic equilibria ($M_p^2 = 0$). Note that no quadratic term as $|\vec{\nabla}u|^2$ appears anymore in (34). Once a solution of this equation is found, the equilibrium can be completely constructed with calculations in the u -space by using (33) and the inverse transformation

$$\psi(u) = \int_0^u (1 - \sigma_d(g) - M_p^2(g))^{-1/2} dg \quad (35)$$

Before continuing to the construction of analytical solutions, we find it convenient to make a normalization by introducing the dimensionless quantities: $\xi = R/R_i$, $\zeta =$

z/R_i , $\tilde{p} = \bar{p}/(B_i^2/\mu_0)$, $\tilde{\rho} = \rho/\rho_i$, $\tilde{u} = u/B_i R_i^2$, $\tilde{I} = I/B_i R_i$, $\tilde{E} = \vec{E}/v_{A_i} B_i$, $\tilde{B} = \vec{B}/B_i$, $\tilde{J} = \vec{J}/(B_i/\mu_0 R_i)$, $\tilde{v} = \vec{v}/v_{A_i}$. The index i can be either a or 0 , where a denotes the magnetic axis, and 0 the geometric center of a configuration. Thus, the normalization constants are defined as follows: R_i is the radial coordinate of the configuration's magnetic axis/geometric center, and B_i , ρ_i , $v_{A_i} = \frac{B_i}{\sqrt{\mu_0 \rho_i}}$ are the magnitude of the magnetic field, the plasma density, and the Afvén velocity thereon. Consequently, with the use of the generalised transformation (33), Eqs. (13)-(15), (20), (28), and (34), are put in the following normalized forms in u -space:

$$\tilde{B} = \tilde{I} \tilde{\nabla} \phi + (1 - \sigma_d - M_p^2)^{-1/2} \tilde{\nabla} \phi \times \tilde{\nabla} \tilde{u} \quad (36)$$

$$\tilde{v} = \frac{M_p}{\sqrt{\tilde{\rho}}} \tilde{B} - \xi^2 (1 - \sigma_d - M_p^2)^{1/2} \left(\frac{d\tilde{\Phi}}{d\tilde{u}} \right) \tilde{\nabla} \phi \quad (37)$$

$$\begin{aligned} \tilde{J} = & \left[(1 - \sigma_d - M_p^2)^{-1/2} \tilde{\Delta}^* \tilde{u} - \frac{1}{2} (1 - \sigma_d - M_p^2)^{-3/2} \frac{d}{d\tilde{u}} (1 - \sigma_d - M_p^2) |\tilde{\nabla} \tilde{u}|^2 \right] \tilde{\nabla} \phi \\ & - \tilde{\nabla} \phi \times \tilde{\nabla} \tilde{I} \end{aligned} \quad (38)$$

$$\tilde{X} = (1 - \sigma_d - M_p^2) \left[\tilde{I} + \xi^2 \left(\frac{d\tilde{F}}{d\tilde{u}} \right) \left(\frac{d\tilde{\Phi}}{d\tilde{u}} \right) \right] \quad (39)$$

$$\tilde{p} = \tilde{p}_s(\tilde{u}) - \tilde{\rho} \left[\frac{\tilde{v}^2}{2} - (1 - \sigma_d) \xi^2 \left(\frac{d\tilde{\Phi}}{d\tilde{u}} \right)^2 \right] \quad (40)$$

and

$$\tilde{\Delta}^* \tilde{u} + \frac{1}{2} \frac{d}{d\tilde{u}} \left(\frac{\tilde{X}^2}{1 - \sigma_d - M_p^2} \right) + \xi^2 \frac{d\tilde{p}_s}{d\tilde{u}} + \frac{\xi^4}{2} \frac{d}{d\tilde{u}} \left[(1 - \sigma_d) \tilde{\rho} \left(\frac{d\tilde{\Phi}}{d\tilde{u}} \right)^2 \right] = 0 \quad (41)$$

where $\tilde{\Delta}^* = \frac{\partial^2}{\partial \xi^2} + \frac{\partial^2}{\partial \zeta^2} - \frac{1}{\xi} \frac{\partial}{\partial \xi}$. In section III for appropriate choices of the surface functions, Eq. (41) will be linearised and solved analytically.

C. Plasma beta and safety factor

The safety factor, measuring the rate of change of toroidal flux with respect to poloidal flux through an infinitesimal annulus between two neighboring flux surfaces, is given by the following expression

$$q \equiv \frac{d\psi_{tor}}{d\psi_{pol}} = \frac{1}{2\pi} \oint \frac{I dl}{R |\tilde{\nabla} \psi|} \quad (42)$$

Expressing the length element dl in Shafranov coordinates (r, θ) [28] the above formula becomes

$$q = \frac{1}{2\pi} \int_0^{2\pi} \frac{I \sqrt{r^2 + \left(\frac{\psi_\theta}{\psi_r}\right)^2}}{R |\vec{\nabla} \psi|} d\theta \quad (43)$$

where, $\psi_\theta = \frac{\partial \psi}{\partial \theta}$, and $\psi_r = \frac{\partial \psi}{\partial r}$. On the basis of the generalised transformation (33) and the adopted normalization, Eq. (43) is put in the following form

$$q = \frac{1}{2\pi} \int_0^{2\pi} \frac{\tilde{I}(\tilde{u}, \xi) \sqrt{\tilde{r}^2 + \left(\frac{\tilde{u}_\theta}{\tilde{u}_r}\right)^2}}{(1 - \sigma_d - M_p^2)^{-1/2} \xi |\vec{\nabla} \tilde{u}|} d\theta \quad (44)$$

from which we can calculate numerically the safety factor profile.

For the local value of the safety factor on the magnetic axis there exists the simpler analytic expression

$$q_a = (1 - \sigma_d - M_p^2)^{1/2} \frac{\tilde{I}}{\xi} \left\{ \frac{\partial^2 \tilde{u}}{\partial \xi^2} \frac{\partial^2 \tilde{u}}{\partial \zeta^2} \right\}_{\xi=\xi_a, \zeta=\zeta_a}^{-1/2} \quad (45)$$

obtained by expansions of the flux function close to the magnetic axis. From equations (39) and (45), one observes that when the flow is parallel to the magnetic field, $\frac{d\Phi}{du} = 0$, then the value of q_a has no dependence on the anisotropy. Indeed q_a becomes independent on σ_{da} , where σ_{da} is the local value of the anisotropy function on the magnetic axis, $\sigma_{da} = \sigma_d|_{R=R_a, z=z_a}$.

In the case of anisotropic pressure we represent the plasma pressure by the effective pressure, so that the plasma beta can be defined as

$$\beta \equiv \frac{\bar{p}}{B^2/2\mu_0} \quad (46)$$

It also useful to define separate toroidal and poloidal quantities β measuring confinement efficiency of each component of the magnetic field. The toroidal beta to be used here is

$$\beta_t = \frac{\bar{p}}{B_0^2/2\mu_0} \quad (47)$$

Recent experiments on the National Spherical Torus Experiment (NSTX) have made significant progress in reaching high toroidal beta $\beta_t \leq 35\%$ [29], while on ITER the beta parameter is expected to take low values, $\beta_t \sim 2\%$ [30].

III. ANALYTIC EQUILIBRIUM SOLUTIONS

A. Solovev-like solution

According to the Solovev ansatz, the free function terms in the GGS equation are chosen to be linear in \tilde{u} as

$$\begin{aligned}\tilde{p}_s &= \tilde{p}_{s_a} \left(1 - \frac{\tilde{u}}{\tilde{u}_b}\right), \quad \tilde{u} \geq 0 \\ \frac{\tilde{X}^2}{1 - \sigma_d - M_p^2} &= \frac{2\epsilon\tilde{p}_{s_a}}{(1 + \delta^2)} \frac{\tilde{u}}{\tilde{u}_b} + 1 \\ \tilde{\rho}(1 - \sigma_d) \left(\frac{d\tilde{\Phi}}{d\tilde{u}}\right)^2 &= \frac{2\lambda\tilde{p}_{s_a}}{(1 + \delta^2)} \left(1 - \frac{\tilde{u}}{\tilde{u}_b}\right)\end{aligned}\quad (48)$$

Here, a denotes the magnetic axis and b the plasma boundary; δ determines the elongation of the magnetic surfaces near the magnetic axis; for $\epsilon > 0$ (< 0) the plasma is diamagnetic (paramagnetic); and λ is a non-negative parameter related with the non-parallel component of the flow. In addition, we impose that the solution \tilde{u} vanishes on the magnetic axis, $\tilde{u}_a = 0$.

With this linearising ansatz the GGS equation (41) reduces to

$$\tilde{\Delta}^* \tilde{u} + \frac{\tilde{p}_{s_a}}{\tilde{u}_b} \left[\frac{\epsilon}{(1 + \delta^2)} - \xi^2 - \xi^4 \frac{\lambda}{(1 + \delta^2)} \right] = 0 \quad (49)$$

which admits the following generalised Solovev solution valid for arbitrary $\tilde{\rho}$, σ_d and M_p^2 :

$$\tilde{u}(\xi, \zeta) = \frac{\tilde{p}_{s_a}}{2(1 + \delta^2)\tilde{u}_b} \left[\zeta^2(\xi^2 - \epsilon) + \frac{\delta^2 + \lambda}{4}(\xi^2 - 1)^2 + \frac{\lambda}{12}(\xi^2 - 1)^3 \right] \quad (50)$$

This solution does not include enough free parameters to impose desirable boundary conditions, but has the property that a separatrix is spontaneously formed. Thus, we can predefine the position of the magnetic axis, ($\xi_a = 1, \zeta_a = 0$), chosen as normalization point and the plasma extends from the magnetic axis up to a closed magnetic surface which we will choose to coincide with the separatrix.

For an up-down symmetric (about the midplane $\zeta = 0$) magnetic surface, its shape can be characterized by four parameters, namely, the ξ coordinates of the innermost and outermost points on the midplane, ξ_{in} and ξ_{out} , and the (ξ, ζ) coordinates of the highest (upper) point of the plasma boundary, (ξ_{up}, ζ_{up}) (see Fig. 14). In terms of these four parameters we can define the normalized major radius

$$\xi_0 = \frac{\xi_{in} + \xi_{out}}{2} \quad (51)$$

which is the radial coordinate of the geometric center, the minor radius

$$\tilde{\alpha} = \frac{\xi_{out} - \xi_{in}}{2} \quad (52)$$

the triangularity of a magnetic surface

$$t = \frac{\xi_0 - \xi_{up}}{\tilde{\alpha}} \quad (53)$$

defined as the horizontal distance between the geometric center and the highest point of the magnetic surface normalized with respect to minor radius, and the elongation of a magnetic surface

$$\kappa = \frac{\zeta_{up}}{\tilde{\alpha}} \quad (54)$$

Usually, we specify the values of R_0 , α , t , and κ , instead of $(\xi_{in}, \xi_{out}, \xi_{up}, \zeta_{up})$ to characterize the shape of the outermost magnetic surface. On the basis of solution (50) the latter quantities can be expressed in terms of ϵ , δ , λ . Subsequently, in order to make an estimate of realistic values for the free parameters ϵ , δ and the radial coordinate of the magnetic axis R_a in connection with the tokamaks under consideration, we employ the relations (51)-(54) to find $(\epsilon, \delta$ and $R_a)$ in terms of the known parameters $(R_0, \alpha, t$ and $\kappa)$. (For ITER: $R_0 = 6.2 m$, $\alpha = 2.0 m$, $\kappa = 1.7$, $t = 0.33$ / for NSTX: $R_0 = 0.85 m$, $\alpha = 0.67 m$, $\kappa = 2.2$, $t = 0.5$). In the static limit ($\lambda = 0$) this estimation procedure can be performed analytically and when the plasma is diamagnetic we find

$$\begin{aligned} \epsilon &= \frac{(R_0 - \alpha)^2}{R_0^2 + \alpha^2} \\ \delta &= \kappa \sqrt{\frac{\alpha}{R_0}} \\ R_a &= \sqrt{R_0^2 + \alpha^2} \end{aligned} \quad (55)$$

Also, for a diamagnetic equilibrium it holds $t = 1$ (cf. Fig. 1). The respective relations for a paramagnetic equilibrium [31] for which $\xi_{in} = 0$ are

$$\begin{aligned} \epsilon &= \frac{(t - 1)^4}{4(t^2 - 2t - 1)} \\ \delta &= \frac{\kappa \sqrt{2}}{\sqrt{-t^2 + 2t + 1}} \\ R_a &= \sqrt{2} R_0 \end{aligned} \quad (56)$$

Relations (55)-(56) will also be employed to assign values of the free parameters ϵ , δ and R_a for non parallel flows ($\lambda \neq 0$) because in this case the above estimation procedure becomes complicated. Afterwards, since the vacuum magnetic field at the geometric center of a configuration is known (ITER: $B_0 = 5.3 T$ / NSTX: $B_0 = 0.43 T$), we can also estimate its value on the magnetic axis by using the relation $B_a = B_0 \frac{R_0}{R_a}$, and therefore the value of \tilde{p}_{s_a} from the relation $\tilde{p}_{s_a} = \frac{\bar{p}_{s_a}}{B_a^2/\mu_0}$, once the maximum pressure for each device is known (ITER: $\sim 10^6 Pa$ / NSTX: $\sim 10^4 Pa$).

Thus, we can fully determine the solution \tilde{u} from Eq. (50), as well as the position of the characteristic points of the boundary and obtain the ITER-like and NSTX-like, diamagnetic and paramagnetic configurations, whose poloidal cross-section with a set of magnetic surfaces are shown in Figs. (1)-(3).

We note that by expansions around the magnetic axis it turns out that the magnetic surfaces in the vicinity of the magnetic axis have elliptical cross-sections (see also [32]-[33]). In the diamagnetic configurations presented in Figs. (1) and (2) the inner part of the separatrix is defined by the vertical line $\xi = \sqrt{\epsilon}$, and, for the NSTX it is located very close to the

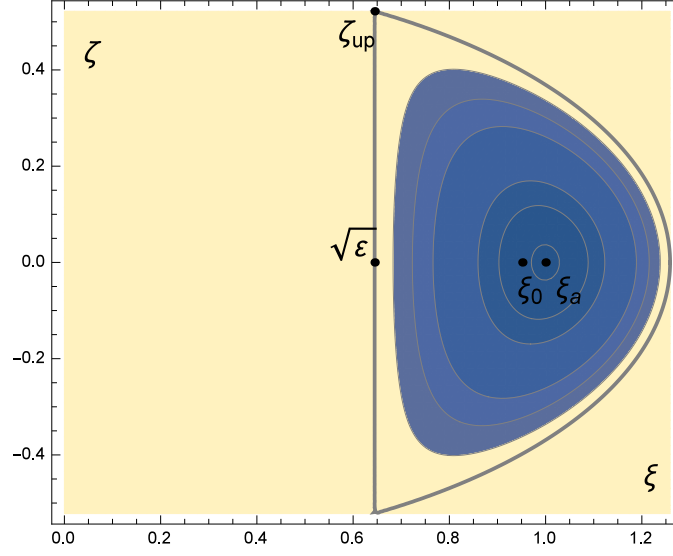


Figure 1: *The static or parallel flow diamagnetic configuration ($\lambda = 0$) with ITER-like characteristics corresponding to $\epsilon = 0.42$, $\delta = 0.97$, $\tilde{p}_{s_a} = 0.049$, $\xi_0 = 0.95$, $\xi_{in} = 0.64$, $\xi_{out} = 1.26$ and $\tilde{\alpha} = 0.32$.*

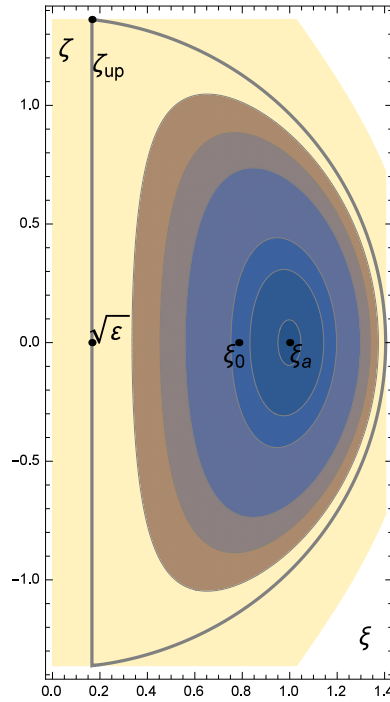


Figure 2: *The static or parallel flow diamagnetic configuration ($\lambda = 0$) with NSTX-like characteristics corresponding to $\epsilon = 0.03$, $\delta = 1.95$, $\tilde{p}_{s_a} = 0.11$, $\xi_0 = 0.78$, $\xi_{in} = 0.17$, $\xi_{out} = 1.40$ and $\tilde{\alpha} = 0.62$.*

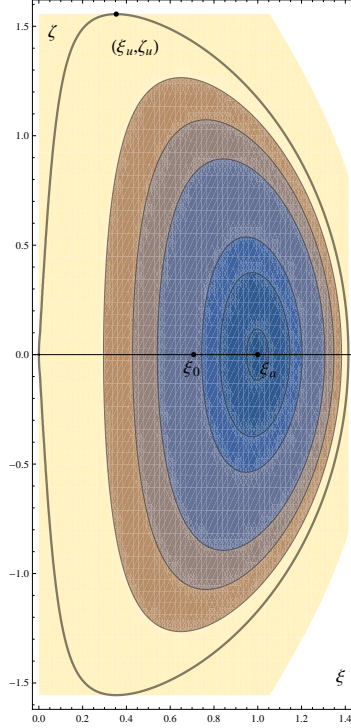


Figure 3: *The static or parallel flow paramagnetic configuration ($\lambda = 0$) with NSTX-like characteristics corresponding to $\epsilon = -0.0089$, $\delta = 2.35$, $\tilde{p}_{s_a} = 0.136$, $\xi_0 = 1/\sqrt{2}$, $\xi_{in} = 0$, $\xi_{out} = \sqrt{2}$ and $\alpha = 0.85 m$.*

tokamak axis of symmetry in accordance with the small hole of spherical tokamaks. It may be noted that such D-shaped configurations are advantageous for improving stability with respect to the interchange modes because of the smaller curvature on the high field side. On the other hand, in a paramagnetic configuration the plasma reaches through a corner the axis of symmetry implying values for the minor radius different from the actual ones, and thus, such a configuration is not typical for conventional tokamaks. However, a configuration with a similar corner was observed recently in the QUEST spherical tokamak as a self organized state [34] (Fig. 5 therein).

B. Hergner-Maschke-like solution

Since the charged particles move parallel to the magnetic field free of magnetic force, parallel flows is a plausible approximation. In particular for tokamaks this is compatible with the fact that the toroidal magnetic field is an order of magnitude larger than the poloidal one and the same scaling is valid for the toroidal and poloidal components of the fluid velocity. Also, for parallel flows the problem remains analytically tractable and leads to a generalised Hergner-Maschke solution to be constructed below.

In the absence of the electric field term (ξ^4 -term) the GGS equation (41) becomes

$$\widetilde{\Delta}^* \widetilde{u} + \frac{1}{2} \frac{d}{d\widetilde{u}} \left(\frac{\widetilde{X}^2}{1 - \sigma_d - M_p^2} \right) + \xi^2 \frac{d\widetilde{p}_s}{d\widetilde{u}} = 0 \quad (57)$$

where all quantities have now been normalized with respect to the geometric center. Choosing the free function terms of Eq. (57) to be quadratic in \widetilde{u} as

$$\begin{aligned} \widetilde{p}_s(\widetilde{u}) &= \widetilde{p}_2 \widetilde{u}^2 \\ \frac{\widetilde{X}^2(\widetilde{u})}{1 - \sigma_d(\widetilde{u}) - M_p^2(\widetilde{u})} &= 1 + \widetilde{X}_1 \widetilde{u}^2 \end{aligned} \quad (58)$$

it reduces to the following linear differential equation

$$\frac{\partial^2 \widetilde{u}}{\partial \xi^2} + \frac{\partial^2 \widetilde{u}}{\partial \zeta^2} - \frac{1}{\xi} \frac{\partial \widetilde{u}}{\partial \xi} + \widetilde{X}_1 \widetilde{u} + 2\widetilde{p}_2 \xi^2 \widetilde{u} = 0 \quad (59)$$

The values of the parameters \widetilde{p}_2 and \widetilde{X}_1 , will be chosen in connection with realistic shaping and values of the equilibrium figures of merit, i.e. the local toroidal beta and the safety factor on the magnetic axis. The solution to Eq. (59) is found by separation of variables,

$$\widetilde{u}(\xi, \zeta) = G(\xi)T(\zeta) \quad (60)$$

on the basis of which, it further reduces to the following form

$$\frac{1}{T(\zeta)} \frac{d^2 T(\zeta)}{d\zeta^2} = -\frac{1}{G(\xi)} \frac{d^2 G(\xi)}{d\xi^2} + \frac{1}{\xi G(\xi)} \frac{dG(\xi)}{d\xi} - \widetilde{X}_1 - 2\widetilde{p}_2 \xi^2 = -\eta^2 \quad (61)$$

where η is the separation constant.

Therefore, the problem reduces to a couple of ODEs. The one for the function T is

$$\frac{d^2 T(\zeta)}{d\zeta^2} + \eta^2 T(\zeta) = 0 \quad (62)$$

having the general solution

$$T(\zeta) = a_1 \cos(\eta\zeta) + a_2 \sin(\eta\zeta) \quad (63)$$

with the coefficients a_1 and a_2 to be determined later. The second equation satisfied by the function G is

$$\frac{d^2 G(\xi)}{d\xi^2} - \frac{1}{\xi} \frac{dG(\xi)}{d\xi} + (\widetilde{X}_1 - \eta^2)G(\xi) + 2\widetilde{p}_2 \xi^2 G(\xi) = 0 \quad (64)$$

Introducing the parameters $\gamma = \widetilde{X}_1$, $\delta = 2\widetilde{p}_2$, and $\varrho = i\sqrt{\delta}\xi^2$, so that $\frac{\partial}{\partial \xi} = 2i\sqrt{\delta}\xi \frac{\partial}{\partial \varrho}$ and $\frac{\partial^2}{\partial \xi^2} = 2i\sqrt{\delta} \frac{\partial}{\partial \varrho} + 4i\sqrt{\delta}\varrho \frac{\partial^2}{\partial \varrho^2}$, Eq. (64) becomes

$$\frac{d^2 G(\varrho)}{d\varrho^2} + \left[i\frac{\eta^2 - \gamma}{4\sqrt{\delta}} \frac{1}{\varrho} - \frac{1}{4} \right] G(\varrho) = 0 \quad (65)$$

Furthermore, if we set $\nu \equiv i\frac{\eta^2 - \gamma}{4\sqrt{\delta}}$ then Eq. (65) is put in the form

$$\frac{d^2 G(\varrho)}{d\varrho^2} + \left[\frac{\nu}{\varrho} - \frac{1}{4} \right] G(\varrho) = 0 \quad (66)$$

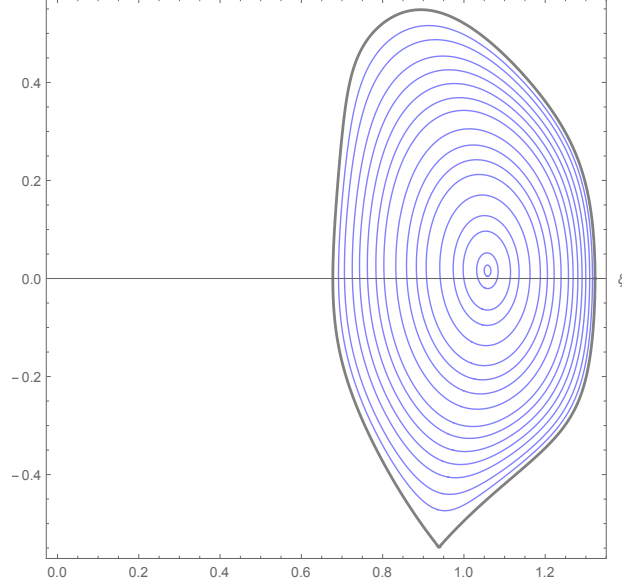


Figure 4: *The poloidal cross-section for an ITER-like diamagnetic equilibria with a lower X-point on the basis of Hernegger-Maschke solution.*

which is a special case of the Whittaker's equation for $\mu = \frac{1}{2}$, and thus, it admits the general solution

$$G(\varrho) = b_1 M_{\nu, \frac{1}{2}}(\varrho) + b_2 W_{\nu, \frac{1}{2}}(\varrho) \quad (67)$$

Here, $M_{\nu, \mu}$ and $W_{\nu, \mu}$ are the Whittaker functions, which are independent solutions of the homonomous differential equation. Consequently, a typical solution of the original equation (59) is written in the form

$$\tilde{u}(\varrho, \zeta) = \left[b_1 M_{\nu, \frac{1}{2}}(\varrho) + b_2 W_{\nu, \frac{1}{2}}(\varrho) \right] [a_1 \cos(\eta\zeta) + a_2 \sin(\eta\zeta)] \quad (68)$$

For further treatment it is convenient to restrict the separation constant η to positive integer values j . Therefore, by superposition the solution can be expressed as

$$\tilde{u}(\varrho, \zeta) = \sum_{j=1}^{\infty} \left[a_j M_{\nu_j, \frac{1}{2}}(\varrho) \cos(j\zeta) + b_j M_{\nu_j, \frac{1}{2}}(\varrho) \sin(j\zeta) + c_j W_{\nu_j, \frac{1}{2}}(\varrho) \cos(j\zeta) + d_j W_{\nu_j, \frac{1}{2}}(\varrho) \sin(j\zeta) \right] \quad (69)$$

Following the analysis given in Appendix A we fully specify the solution (69) and construct the diverted equilibrium with ITER-like characteristics shown in Fig. (4). Note that the magnetic axis is located outside of the midplane $\zeta = 0$ at $(\xi_a = 1.05815, \zeta_a = 0.0159088)$.

In a similar way we constructed NSTX-Upgrade-like equilibria ($R_0 = 0.93 m$, $\alpha = 0.57 m$, $B_0 = 1.0 T$, $\kappa = 2.5$, and $t = 0.3$) on the basis of the extended Hernegger-Maschke solution, shown in Fig. (5). The magnetic axis of the respective configuration is located at the position $(\xi_a = 1.19012, \zeta_a = 0.0511745)$, while the flux function on axis takes the value $\tilde{u}_a^* = 0.948259$.

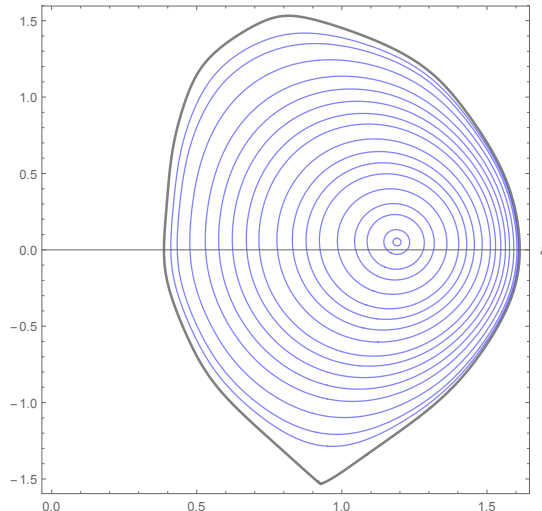


Figure 5: An NSTX-U-like diamagnetic equilibrium configuration for values of the free

$$\text{parameters } \tilde{p}_2 = 4.825, \tilde{X}_1 = -0.65.$$

IV. EFFECTS OF ANISOTROPY AND FLOW ON EQUILIBRIUM

To completely determine the equilibrium we choose the plasma density, the Mach function and the anisotropy function profiles to be peaked on the magnetic axis and vanishing on the plasma boundary. Specifically, for the Solovév solution we choose: $\tilde{\rho}(\tilde{u}) = \tilde{\rho}_a \left(1 - \frac{\tilde{u}}{\tilde{u}_b}\right)^{1/2}$, $M_p^2(\tilde{u}) = M_{p_a}^2 \left(1 - \frac{\tilde{u}}{\tilde{u}_b}\right)^\mu$ and $\sigma_d(\tilde{u}) = \sigma_{d_a} \left(1 - \frac{\tilde{u}}{\tilde{u}_b}\right)^n$ with $\tilde{\rho}_a$ and \tilde{u}_b constant quantities, while for the Hernegger-Maschke solution we choose: $\tilde{\rho}(\tilde{u}) = \tilde{\rho}_a \left(\frac{\tilde{u}}{\tilde{u}_a}\right)^{1/2}$, $M_p^2(\tilde{u}) = M_{p_a}^2 \left(\frac{\tilde{u}}{\tilde{u}_a}\right)^\mu$, $\sigma_d(\tilde{u}) = \sigma_{d_a} \left(\frac{\tilde{u}}{\tilde{u}_a}\right)^n$, with $\tilde{\rho}_a$ and \tilde{u}_a constant quantities, respectively. It is noted here that the above chosen density function, peaked on the magnetic axis and vanishing on the boundary is typical for tokamaks. Also, the Mach function adopted having a similar shape is reasonable at least in connection with experiments with on axis focused external momentum sources. The functions $\tilde{\rho}$, M_p^2 and σ_d chosen depend on two free parameters; their maximum on axis and an exponent associated with the shape of the profile; the exponent of the function M_p^2 , connected with flow shear, is held fixed at $\mu = 2$.

The value of $M_{p_a}^2$ depends on the kind of tokamak (conventional or spherical). On account of experimental evidence [35, 36], the toroidal rotation velocity in tokamaks is approximately $10^4 - 10^6 \text{ ms}^{-1}$ which for large conventional ones implies $M_{p_a}^2 \sim 10^{-4}$, while the flow is stronger for spherical tokamaks ($M_{p_a}^2 \sim 10^{-2}$) [29]. In addition, from the requirement of positiveness for all pressures within the whole plasma region, we find that the pressure anisotropy parameter σ_{d_a} takes higher values on spherical tokamaks than in the conventional ones, as shown on Table I; also it must be $n \geq 2$. An argument why the flow and pressure anisotropy are stronger in spherical tokamaks is that in this case the magnetic field is strongly inhomogeneous, as the aspect ratio is too small. In contrast, for the generalised Hernegger-Maschke equilibrium the pressure anisotropy takes a little higher values on ITER rather than on the NSTX-U tokamak, and this may be attributed to a peculiarity of this solution.

When the plasma is diamagnetic the toroidal magnetic field inside the plasma decreases

	Diamagnetic		Paramagnetic	
	ITER	NSTX	ITER	NSTX
Parallel flow ($\lambda = 0$)	0.08	0.11	0.089	0.12
Non-parallel flow ($\lambda = 0.5$)	0.10	0.13	0.094	0.13

Table I: *Approximate maximum permissible values of the free parameter σ_{da} for the extended Solovév solution in connection with the non-negativeness of pressure.*

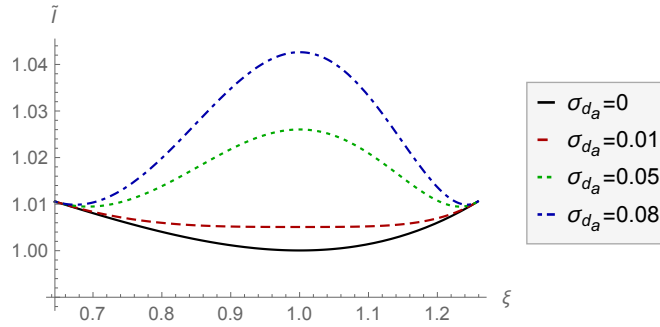


Figure 6: *The paramagnetic action of pressure anisotropy through the parameter σ_{da} on diamagnetic ITER-like equilibria with field-aligned flow, on the midplane $\zeta = 0$, for the extended Solovév solution. This result also holds for Hernegger-Maschke-like equilibria and paramagnetic plasmas, as well as for non-parallel flow.*

from its vacuum value, and consequently the profile of the function \tilde{I} is expected to be hollow ($\tilde{B}_\phi = \frac{\tilde{I}}{\xi}$). As shown in Fig. (6), as σ_{da} becomes larger the field increases, and for sufficient high σ_{da} it becomes peaked on the magnetic axis. This means that increasing pressure anisotropy acts paramagnetically in terms of its maximum value on axis, σ_{da} . Additionally, plasma flow through M_{pa}^2 also acts paramagnetically, but its effects are weaker than that of pressure anisotropy, as shown in Fig. (7). On the other side, pressure anisotropy may also act diamagnetically through the shaping parameter n when σ_{da} is fixed [cf. Fig. (8)].

For the extended diamagnetic Solovév solution, in the static and isotropic case the toroidal current density monotonically increases from ξ_{in} to ξ_{out} :

$$\tilde{J}_\phi = 1.548\xi - \frac{0.333}{\xi} \quad (70)$$

When anisotropy is present, there are three regions where \tilde{J}_ϕ displays different behavior: for $\xi_{in} < \xi < \xi_1$ and $\xi_2 < \xi < \xi_{out}$ it decreases, while for $\xi_1 < \xi < \xi_2$ it increases, compared with the isotropic case, as shown in Fig. (9). When the plasma is paramagnetic, \tilde{J}_ϕ sharply falls off near the axis of symmetry, and then behaves diamagnetic-like. In contrast, the extended

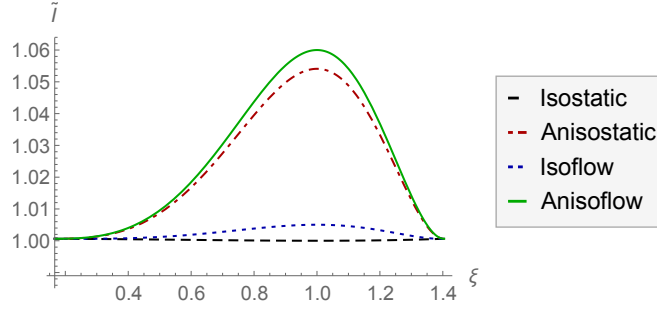


Figure 7: *The additive paramagnetic action of anisotropy and flow on NSTX-like diamagnetic equilibria, on the midplane $\zeta = 0$. We note that anisotropy (red-dashed-dotted curve) has a stronger impact than the flow (Blue Dotted curve) on equilibrium. The maximum paramagnetic action is found when both anisotropy and flow are present (green-straight curve).*

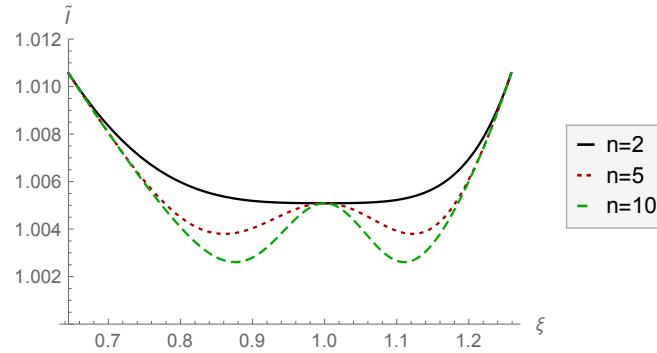


Figure 8: *Raising the free parameter n of the anisotropy function, decreases the toroidal magnetic field in the off-axis region, leading to a diamagnetic action.*

Hernegger-Maschke solution has a more realistic \tilde{J}_ϕ profile peaked on the magnetic axis and vanishing on the boundary. In this case \tilde{J}_ϕ slightly increases with anisotropy.

Furthermore, in the presence of pressure anisotropy the poloidal component \tilde{J}_ζ of the Solovev and the radial \tilde{J}_ξ of the Hernegger-Maschke solution, present two extrema on the plane ($\zeta = \zeta_a$) containing the magnetic axis with their absolute values to be increasing with σ_{da} [Fig. (10)]. For fixed σ_{da} , the higher n is the closer to the magnetic axis are located the extrema.

The Solovev toroidal velocity is expressed as

$$\tilde{v}_\phi = \frac{\tilde{I} M_p}{\xi \sqrt{\tilde{\rho}}} - \xi \sqrt{1 - \frac{M_p^2}{1 - \sigma_d} \left(\frac{2\lambda \tilde{p}_{s_a}}{\tilde{\rho}(1 + \delta^2)} \left(1 - \frac{\tilde{u}}{\tilde{u}_b} \right) \right)^{1/2}} \quad (71)$$

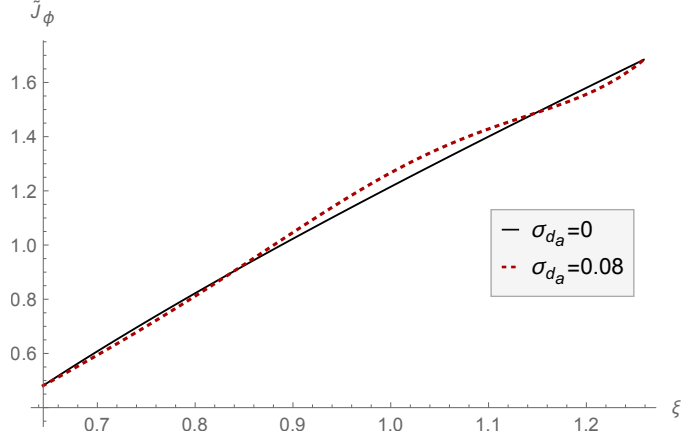


Figure 9: *Diamagnetic ITER-like $\tilde{J}_\phi(\sigma_{d_a})$ on the midplane $\zeta = 0$, for $\lambda = 0$, on the basis of the Solovév-like solution. For non-parallel flow the intersection points are displaced a little closer to the magnetic axis.*

Thus, for parallel flow the second term in Eq. (71) vanishes and \tilde{v}_ϕ behaves like \tilde{I} as concerns its dependence on $M_{p_a}^2$, σ_{d_a} and n . We can see the increase of the maximum value of the toroidal velocity with σ_{d_a} , displaced on the left side of the magnetic axis, in Fig. (11), for an ITER-like diamagnetic configuration. For the NSTX the impact of anisotropy on \tilde{v}_ϕ is qualitatively similar but quantitatively slightly stronger because of the higher values of σ_{d_a} . This behavior holds for the Hernegger-Maschke-like solution. For non parallel flow \tilde{v}_ϕ changes sign because of the negative second term in Eq. (71).

When the plasma is paramagnetic \tilde{v}_ϕ reverses near the axis of symmetry and then behaves as the diamagnetic one to the right of the reversal point, as shown in Fig. (12). In spherical tokamaks the reversal point is displaced closer to the magnetic axis and \tilde{v}_ϕ remains positive in a larger region than in the conventional ITER-like one. Reversal of \tilde{v}_ϕ during the transition to improved confinement regimes have been observed in ASDEX Upgrade [37] and in LHD [38].

Pressure anisotropy has an appreciable impact on the various pressures, with \tilde{p}_\parallel increasing, while \tilde{p}_\perp and $\langle \tilde{p} \rangle$ decreasing with σ_d as expected by Eqs. (10)-(12). For a Solovév-like diamagnetic equilibrium the ratio of the scalar pressures parallel and perpendicular to the magnetic field is approximately equal for the two kinds of tokamak: $\left(\frac{\tilde{p}_\parallel}{\tilde{p}_\perp}\right)_{ITER} \approx 1.227$, $\left(\frac{\tilde{p}_\parallel}{\tilde{p}_\perp}\right)_{NSTX} \approx 1.099$. In addition, the ratio of the maximum values of the average pressures for these two tokamaks is $\frac{\langle \tilde{p} \rangle_{NSTX}}{\langle \tilde{p} \rangle_{ITER}} \approx 2.17$. For a Hernegger-Maschke-like diamagnetic equilibrium, the respective ratios are: $\left(\frac{\tilde{p}_\parallel}{\tilde{p}_\perp}\right)_{NSTX-U} \approx 1.08$ and $\left(\frac{\tilde{p}_\parallel}{\tilde{p}_\perp}\right)_{ITER} \approx 1.5$. Also, for this equilibrium we found $\frac{\langle \tilde{p} \rangle_{NSTX-U}}{\langle \tilde{p} \rangle_{ITER}} \approx 2.73$, a ratio that approaches the respective Solovév one.

As expected by Eqs. (11) and (12) the flow has a slightly stronger impact on \tilde{p} than pressure anisotropy, as also shown in Fig. (13). At last, the rest of the equilibrium quantities and confinement figures of merit as the local toroidal beta on axis and the safety factor are almost insensitive to anisotropy.

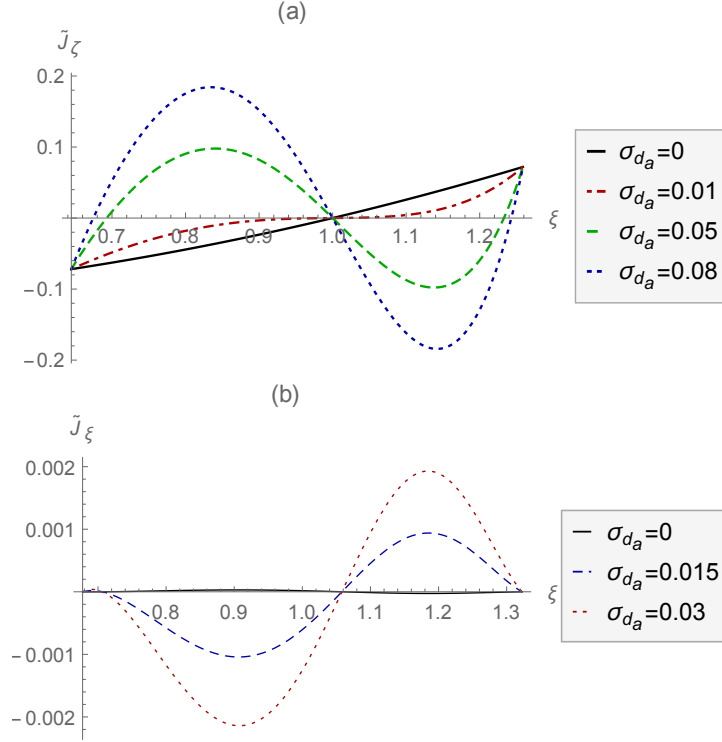


Figure 10: Variation of the poloidal components of current density for ITER-like diamagnetic equilibria in the presence of pressure anisotropy: (a) \tilde{J}_ζ on the midplane $\zeta = 0$ on the basis of the extended Solovév solution, (b) \tilde{J}_ξ on the plane $\zeta = \zeta_a$ on the basis of the extended Hérnegger-Maschke solution.

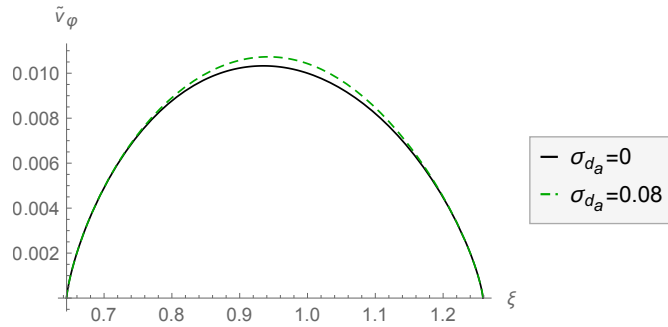


Figure 11: Diamagnetic ITER-like $\tilde{v}_\phi(\sigma_{d_a})$ profile for $\lambda = 0$.

V. CONCLUSIONS

A generalised Grad-Shafranov equation [Eq. (29)] governing axisymmetric plasma equilibria in the presence of pressure anisotropy and incompressible flow was derived. This equation recovers known GS-like equations governing static anisotropic equilibria and isotropic equi-

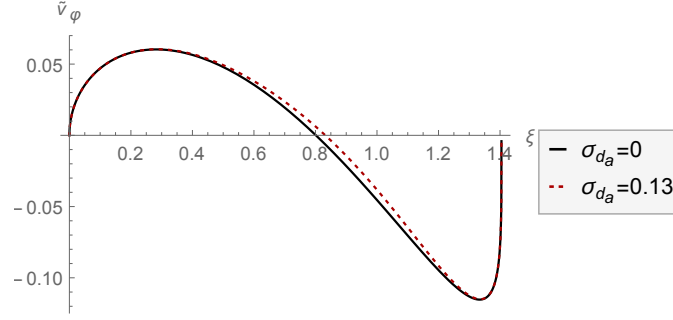


Figure 12: Paramagnetic \tilde{v}_ϕ on the midplane $\zeta = 0$ for NSTX-like equilibria with non-parallel flow for $\lambda = 0.5$.

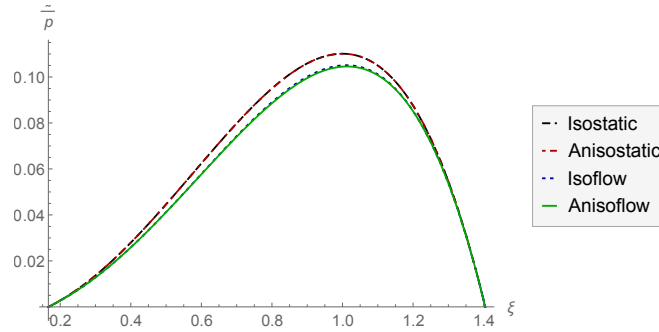


Figure 13: The influence of pressure anisotropy against the flow on \tilde{p} on the midplane $\zeta = 0$, for the NSTX diamagnetic equilibria with parallel flow ($\lambda = 0$). When the flow is present the overall effective pressure decreases from its static value, while the presence of pressure anisotropy does not have an important effect on it. The maximum attainable values for the parameters M_p^2 and σ_{da} used are imposed by the non-negativeness of pressure.

libria with plasma flow. Also for static isotropic equilibria the equation is reduced to the usual well known GS equation. The derivation was based on a diagonal pressure tensor with one element parallel to the magnetic field, p_{\parallel} , and two equal perpendicular ones, p_{\perp} . As a measure of the pressure anisotropy we introduced the function $\sigma_d = \mu_0 \frac{p_{\parallel} - p_{\perp}}{B^2}$, assumed to be uniform on magnetic surfaces, while the flow was expressed by the poloidal Alfvénic Mach function $M_p = \frac{v_{pol}}{v_{A_{pol}}}$, where $v_{A_{pol}}$ is the Alfvén velocity. The form of the equation containing the sum $M_p^2 + \sigma_d$ indicates that pressure anisotropy and flow act additively with the only exception the electric field term. In addition we derived a generalised Bernoulli equation [Eq. (28)] involving the effective isotropic pressure $\bar{p} = \frac{p_{\parallel} + p_{\perp}}{2}$.

On the basis of a simpler form of the GGS equation obtained by a generalised transformation, the transformed equation was linearised and solved for appropriate choices of the free functions appearing in it. Specifically, an extended Solovév solution describing configurations

with the plasma boundary coinciding with a separatrix, and an extended Hernerger-Maschke solution with a fixed boundary possessing an X-point imposed by appropriate boundary conditions, were derived. Employing these solutions, ITER, NSTX and NSTX-U-like equilibria for arbitrary flow, both diamagnetic and paramagnetic, were constructed. In addition, we examined the impact of anisotropy -through the parameters σ_{da} and n , defining the maximum value and the shape of the function σ_d - and flow -through the Alfvénic Mach number M_{pa}^2 defining the maximum of the function M_p^2 - on the equilibria constructed and came to the following conclusions.

Pressure anisotropy has a stronger impact on equilibrium than that of the flow because the maximum permissible values of σ_{da} are in general higher than the respective M_{pa}^2 ones, with the effects of the flow to be more noticeable in the spherical tokamaks. In addition, both anisotropy and flow through the parameters σ_{da} and M_{pa}^2 have an additive paramagnetic impact on equilibrium, with stronger paramagnetic effects in spherical tokamaks, while anisotropy through n acts diamagnetically. Furthermore, pressure anisotropy has an appreciable impact on equilibrium quantities such as the current density, the toroidal velocity and the parallel and perpendicular pressures, while \bar{p} is slightly affected by the pressure anisotropy and more by the flow.

On the basis of the GGS obtained in this study one can develop a code to solve the problem for arbitrary choices of the free functions involved in order to deal with experimental equilibrium profiles or extend existing codes, e.g. the isotropic HELENA code for incompressible parallel flows [39]. Also, it is interesting to extend the papers on static equilibria with reversed current density [40]-[44] in the presence of incompressible flow and pressure anisotropy. In addition, the study can be extended for the more general case of helically symmetric equilibria.

Let us finally note that complete understanding of the equilibrium with plasma flow and pressure anisotropy requires substantial additional work in connection with compressibility, alternative potentially more pertinent physical assumptions on the functional dependence of the anisotropy function σ_d and more realistic numerical solutions. However, in these cases the reduced equilibrium equations are expected to be much more complicated compared with the relative simple GGS derived in the present study which contributes to understanding the underlying physics.

ACKNOWLEDGEMENTS

One of the authors (GNT) would like to thank Henri Tasso, George Poulipoulis and Apostolos Kuiroukidis for very useful discussions. This work has been carried out within the framework of the EUROfusion Consortium and has received funding from (a) the National Programme for the Controlled Thermonuclear Fusion, Hellenic Republic, (b) Euratom research and training programme 2014-2018 under grant agreement No 633053. The views and opinions expressed herein do not necessarily reflect those of the European Commission.

Appendix A:

Details for the construction of the diverted equilibrium of Fig. (4)

In order to make the analysis more convenient, we factorize (69) with respect to the coefficient a_1 , so that the system of algebraic equations that will be derived from the imposed boundary conditions to be inhomogeneous and therefore easier to be solved numerically:

$$\tilde{u} = a_1 \left\{ M_{\nu_1, \frac{1}{2}}(\varrho) \cos(\zeta) + \frac{b_1}{a_1} M_{\nu_1, \frac{1}{2}}(\varrho) \sin(\zeta) + \frac{c_1}{a_1} W_{\nu_1, \frac{1}{2}}(\varrho) \cos(\zeta) + \frac{d_1}{a_1} W_{\nu_1, \frac{1}{2}}(\varrho) \sin(\zeta) \right. \\ \left. + \sum_{j=2}^N \left[\frac{a_j}{a_1} M_{\nu_j, \frac{1}{2}}(\varrho) \cos(j\zeta) + \frac{b_j}{a_1} M_{\nu_j, \frac{1}{2}}(\varrho) \sin(j\zeta) + \frac{c_j}{a_1} W_{\nu_j, \frac{1}{2}}(\varrho) \cos(j\zeta) + \frac{d_j}{a_1} W_{\nu_j, \frac{1}{2}}(\varrho) \sin(j\zeta) \right] \right\} \quad (\text{A1})$$

Now, by setting $a_j^* = \frac{a_j}{a_1}$, $b_j^* = \frac{b_j}{a_1}$, $c_j^* = \frac{c_j}{a_1}$, and $d_j^* = \frac{d_j}{a_1}$, then the solution can be expressed as

$$\tilde{u}(\varrho, \zeta) = a_1 \tilde{u}^*(\varrho, \zeta) \quad (\text{A2})$$

where

$$\tilde{u}^*(\varrho, \zeta) = \sum_{j=1}^N \left[a_j^* M_{\nu_j, \frac{1}{2}}(\varrho) \cos(j\zeta) + b_j^* M_{\nu_j, \frac{1}{2}}(\varrho) \sin(j\zeta) + c_j^* W_{\nu_j, \frac{1}{2}}(\varrho) \cos(j\zeta) + d_j^* W_{\nu_j, \frac{1}{2}}(\varrho) \sin(j\zeta) \right] \quad (\text{A3})$$

with $a_1^* = 1$.

An up-down asymmetric boundary consisting of a smooth upper part and a lower part that possesses an X-point, is described by the parametric equations introduced in [45], with its boundary being represented by the following characteristic points shown in Fig. (14):

$$\text{Inner point : } (\xi_{in} = 1 - \frac{\alpha}{R_0}, \zeta_{in} = 0)$$

$$\text{Outer point : } (\xi_{out} = 1 + \frac{\alpha}{R_0}, \zeta_{out} = 0)$$

$$\text{Upper point : } (\xi_{up} = 1 - t \frac{\alpha}{R_0}, \zeta_{up} = \kappa \frac{\alpha}{R_0})$$

$$\text{Lower X-point : } (\xi_x = 1 + \frac{\alpha}{R_0} \cos[\pi - \tan^{-1}(\frac{\kappa}{t})], \zeta_x = -\kappa \frac{\alpha}{R_0})$$

In order to calculate the unknown coefficients of the solution we will impose the condition that \tilde{u}^* vanishes on the boundary. Function \tilde{u}^* is in general complex, and since it satisfies the GGS equation, then both its real and imaginary parts are also solutions of this equation. Here, following Ref. [46] we will work with the imaginary part of the flux function. So the first four conditions are:

$$\text{Im}[\tilde{u}^*(\xi_{in}, \zeta_{in})] = \text{Im}[\tilde{u}^*(\xi_{out}, \zeta_{out})] = \text{Im}[\tilde{u}^*(\xi_{up}, \zeta_{up})] = \text{Im}[\tilde{u}^*(\xi_x, \zeta_x)] = 0 \quad (\text{A4})$$

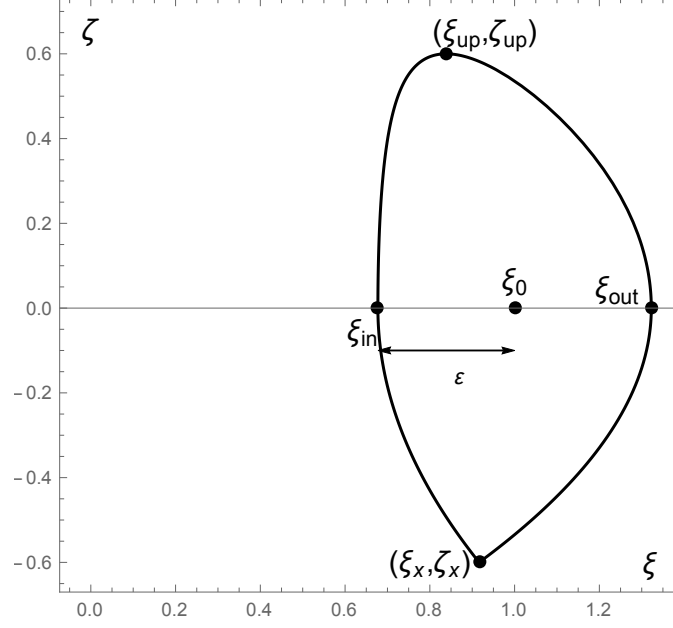


Figure 14: *Characteristic points determining an up-down asymmetric boundary, described by the parametric equations given in [45].*

In addition, five boundary conditions related with the first derivative of these characteristic points are imposed:

$$Im[\tilde{u}_\zeta^*(\xi_{in}, \zeta_{in})] = Im[\tilde{u}_\zeta^*(\xi_{out}, \zeta_{out})] = Im[\tilde{u}_\xi^*(\xi_{up}, \zeta_{up})] = Im[\tilde{u}_\zeta^*(\xi_x, \zeta_x)] = Im[\tilde{u}_\xi^*(\xi_x, \zeta_x)] = 0 \quad (A5)$$

where, $\tilde{u}_\zeta^* = \frac{\partial \tilde{u}^*}{\partial \zeta}$, and $\tilde{u}_\xi^* = \frac{\partial \tilde{u}^*}{\partial \xi}$. The above conditions guarantee smoothness of the curve at the characteristic points; particularly, the curve is imposed to be perpendicular to the midplane. Furthermore, there exist three other conditions introduced in [47], that involve the second derivatives of \tilde{u}^* related with the curvature of the boundary curve in the characteristic points. These are:

$$Im[\tilde{u}_{\zeta\xi}^*(\xi_{up}, \zeta_{up})] = \frac{\kappa}{\varepsilon \cos^2 w_1} Im[\tilde{u}_\zeta^*(\xi_{up}, \zeta_{up})] \quad (A6)$$

$$Im[\tilde{u}_{\zeta\zeta}^*(\xi_{in}, \zeta_{in})] = -\frac{(1-w_1)^2}{\varepsilon \kappa^2} Im[\tilde{u}_\xi^*(\xi_{in}, \zeta_{in})] \quad (A7)$$

$$Im[\tilde{u}_{\zeta\zeta}^*(\xi_{out}, \zeta_{out})] = \frac{(1+w_1)^2}{\varepsilon \kappa^2} Im[\tilde{u}_\xi^*(\xi_{out}, \zeta_{out})] \quad (A8)$$

where the parameter w_1 relates to the triangularity of the boundary, $\sin w_1 = t$. Thus, for ITER-like characteristics, by setting $j_{max} = 4$ and choosing the free parameters $\tilde{p}_2 = 19.5$, $\tilde{X}_1 = -0.3$, by the imposition of the above conditions we find the values for the unknown coefficients presented on Table II.

Coefficient Values			
a_1^*	1	c_1^*	2.2319
a_2^*	-0.625449	c_2^*	-1.82077
a_3^*	0.13783	c_3^*	0.52774
a_4^*	-0.0166821	c_4^*	-0.0657547
b_1^*	11.2021	d_1^*	29.2229
b_2^*	-4.93763	d_2^*	-20.6201
b_3^*	1.23997	d_3^*	10.462
b_4^*	-0.117724	d_4^*	-2.64276

Table II: *Values of the coefficients of the solution \tilde{u}^* for an ITER-like diamagnetic configuration.*

Once the solution $\tilde{u}^*(\rho, \zeta)$ is fully determined, we can find the position of the magnetic axis, by solving the equations $Im[\tilde{u}_\xi^*] = 0$ and $Im[\tilde{u}_\zeta^*] = 0$ located outside of the midplane $\zeta = 0$ at $(\xi_a = 1.05815, \zeta_a = 0.0159088)$. Subsequently, with the aid of Eq. (45) we impose the condition $q_a = 1.1$, just for the Kruskal-Shafranov limit to be satisfied, implementation of which gives $a_1 = 1.07751$. Thus, solution \tilde{u} is fully determined, with its value on axis to be $\tilde{u}_a = -0.0416752$. Closed magnetic surfaces associated with \tilde{u} -contours of the equilibrium configuration are shown in Fig. (4).

REFERENCES

-
- [1] P. H. Diamond, S. I. Itoh, K. Itoh and T. S. Hahm, Plasma Phys. Control. Fusion 47 (2005) R35-R161
 - [2] K. G. McClements and M. J. Hole, Phys. Plasmas 17, (2010) 082509
 - [3] G. F. Chew, M. L. Goldberger, F. E. Low, Proc. R. Soc. London 236 (1956) 112
 - [4] L. S. Solov'ev, Sov. Phys. JETP 26, (1968) 400
 - [5] F. Hergner, in: E. Canobbio et al. (Eds.), Proceedings of the 5th Conference on Control. Fusion,

- Vol. I Commissariat a l' Energie Atomique, Grenoble, 1972, p. 26.; E.K. Maschke, Plasma Phys. 15, (1973) 535
- [6] A. I. Morozov and L. S. Solov'ev, Rev. Plasma Phys. 8 (1980) 1
- [7] E. Hameiri, Phys. Fluids 26 (1983) 230
- [8] H. Tasso, G. N. Throumoulopoulos, Phys. Plasmas 5 (1998) 2378
- [9] R. Courant, D. Hilbert, Methods of mathematical physics (Interscience Publishers, 1966), Vol. 2, p. 372
- [10] C. Mercier, M. Cotsaftis, Nucl. Fusion 1 (1961) 121
- [11] R. A. Clemente, Nucl. Fusion 33 (1993) 963
- [12] W. Zwingmann, L.G. Eriksson and P. Stubberfield, Plasma Phys. Control. Fusion 43 (2001) 1441
- [13] V. D. Pustovitov, Plasma Phys. Control. Fusion 52 (2010) 065001
- [14] N. D. Lepikhin and V. D. Pustovitov, Plasma Physics Reports, 39 (2013) 605
- [15] M. Furukawa, Phys. Plasmas 21 (2014) 012511
- [16] E. A. Kuznetsov, T. Passot, V. P. Ruban, P. L. Sulem, Phys. Plasmas 22 (2015) 042114
- [17] R. Iacono, A. Bondeson, F. Troyon, and R. Gruber, Phys. Fluids B 2 (1990) 1794
- [18] V. I. Ilgisonis, Phys. Plasmas 3 (1996) 4577
- [19] L. Guazzotto, R. Betti, J. Manickam, and S. Kaye, Phys. Plasmas 11, (2004) 604
- [20] R. A. Clemente and D. Sterzo Plasma Phys. Control. Fusion 51 (2009) 085011
- [21] V. D. Pustovitov, AIP Conf. Proc. 1478 (2012) 50
- [22] Z S Qu, M Fitzgerald and M J Hole, Plasma Phys. Control. Fusion 56 (2014) 075007
- [23] A. A. Ivanov, A. A. Martynov, S. Yu. Medvedev and Yu. Yu. Poshekhonov, Plasma Physics Reports, 41 (2015) 203
- [24] G. Poulipoulis, G. N. Throumoulopoulos, H. Tasso, Phys. Plasmas J12, (2005) 042112
- [25] D. Palumbo, Nuovo Cimento B 53 (1968) 507
- [26] D. Palumbo and M. Balzano, Atti Acc. Sc. Lett. Palermo IV(I) (1983-84) 129
- [27] C. Simintzis, G. N. Throumoulopoulos, G. Pantis, H. Tasso, Phys. Plasmas 8 (2001) 2641
- [28] J. P. Freidberg, in Ideal Magnetohydrodynamics (Plenum Press, 1987), ps. 108 and 117
- [29] J. E. Menard, M. G. Bell, R. E. Bell, et al., Nucl. Fusion 43 (2003) 330

- [30] T. C. Luce, C. D. Challis, S. Ide, et al., Nucl. Fusion 54 (2014) 013015
- [31] I. Arapoglou, G. N. Throumoulopoulos, H. Tasso, Phys. Letters A (2013) 310
- [32] L. L. Lao, S. P. Hirshman and R. M. Wieland, Phys. Fluids 24 (1981) 1431
- [33] Joao P. S. Bizarro, Nucl. Fusion 54 (2014) 083015
- [34] Kishore Mishra, H. Zushi, H. Idei, et al., Nucl. Fusion 55 (2015) 083009
- [35] K. Brau, M. Bitter, R. J. Goldston et al., Nucl. Fusion 23 (1983) 1643
- [36] G. N. Throumoulopoulos, G. Pantis, Phys. Fluids B 1 (1989) 1827
- [37] R.M. McDermott, C. Angioni, G. D. Conway, et al., Nucl. Fusion 54 (2014) 043009
- [38] K. Ida, H. Lee, K. Nagaoka, et al., PRL 111 (2013) 055001
- [39] G. Poulipoulis, G.N. Throumoulopoulos, C. Konz and EFDA ITM-TF contributors, “Extending HELENA to equilibria with incompressible parallel plasma rotation”, 39th EPS Conference and 16th Int. Congress on Plasma Physics, Stockholm (2012) P4.027
- [40] S. Wang, Phys. Rev. Lett. 93 (2004) 155007
- [41] P. Rodrigues and Joao P. S. Bizarro, Phys. Rev. Lett. 95 (2005) 015001
- [42] P. Rodrigues and Joao P. S. Bizarro, Phys. Rev. Lett. 99 (2007) 125001
- [43] A. A. Martynov, S. Yu. Medvedev, and L. Villard, Phys. Rev. Lett. 91 (2003) 085004
- [44] Caroline G. L. Martins, M. Roberto, I. L. Caldas, and F. L. Braga, Phys. Plasmas 18 (2011) 082508
- [45] A. Kuiroukidis, G. N. Throumoulopoulos, Plasma Phys. Control. Fusion 57 (2015) 078001
- [46] L. Guazzotto, J. P. Freidberg, Phys. Plasmas 14 (2007) 112508
- [47] A. J. Cerfon, J. P. Freidberg, Phys. Plasmas 17 (2010) 032502